Rashba spin-orbit coupling in InSb nanowires under transverse electric field

X. W. Zhang and J. B. Xia
Institute of Semiconductors, Chinese Academy of Sciences, P.O. Box 912, Beijing 100083, China
(Received 17 April 2006; revised manuscript received 31 May 2006; published 2 August 2006)

We investigate the Rashba spin-orbit coupling brought by transverse electric field in InSb nanowires. In small k_z (k_z is the wave vector along the wire direction) range, the Rashba spin-orbit splitting energy has a linear relationship with k_z, so we can define a Rashba coefficient similarly to the quantum well case. We deduce some empirical formulas of the spin-orbit splitting energy and Rashba coefficient, and compare them with the effective-mass calculating results. It is interesting to find that the Rashba spin-orbit splitting energy decreases as k_z increases when k_z is large due to the k_z-quadratic term in the band energy. The Rashba coefficient increases with increasing electric field, and shows a saturating trend when the electric field is large. As the radius increases, the Rashba coefficient increases at first, then decreases. The effects of magnetic fields along different directions are discussed. The case where the magnetic field is along the wire direction or the electric field direction are similar. The spin state in an energy band changes smoothly as k_z changes. The case where the magnetic field is perpendicular to the wire direction and the electric field direction is quite different from the above two cases, the k_z-positive and negative parts of the energy bands are not symmetrical, and the energy bands with different spins cross at a k_z-nonzero point, where the spin splitting energy and the effective g factor are zero.

DOI: 10.1103/PhysRevB.74.075304 PACS number(s): 73.21.Hb, 72.25.Dc, 73.22.−f, 75.75.+a

I. INTRODUCTION

Nowadays, much of the research in semiconductor physics has been shifting towards spintronics due to its potential extensive applications.[1,2] The electron spin might be used in the future to build quantum computing devices combining logic and storage based on spin-dependent effects in semiconductors. One of the most important spin-based devices was proposed by Datta and Das.[3] Improvements to the original design have been proposed recently by Egues *et al.*[4,5] The Datta-Das device makes use of the Rashba spin-orbit coupling[6–8] in order to perform controlled rotations of a field-effect transistor (FET).[9] The influence of Rashba spin-orbit coupling in quantum wells[9–17] and quantum dots[18–23] has been investigated in a number of theoretical and experimental works.

There is a growing interest and experimental progress in one-dimensional semiconductors called nanowires. Nanowires can be grown out of numerous semiconductor materials by several methods and in a large range of radius.[24–30] They can be used as conducting nanowires to build quantum devices.[28] The transport properties of nanowires have been investigated experimentally.[27] Zhang and Xia[31] studied the electronic structure of nanowires using the six-band effective-mass envelope-function method.

Recently, people pay more attention to the Rashba spin-orbit coupling in nanowires because of its abundance of physical phenomena and application values. The Rashba spin-orbit coupling effect was observed in nanowires.[32] The spin polarization of edge states and the magneto-subband structure in nanowires were studied within the density functional theory in the local spin density approximation.[33] The Rashba spin-orbit splitting[34–40] and spin-polarized transport properties[41–43] of nanowires and quantum networks built of nanowires,[44] and the combined effect of magnetic field[45–51] were studied theoretically by adding a k-linear Rashba term in the Hamiltonian equation. We know that the Rashba spin-orbit coupling is caused by the structure inversion asymmetry (SIA), which can be introduced by an external electric field. As a result, we can study the Rashba effect in the case where the nanowires are in the presence of electric field, without adding a k-linear Rashba term empirically.

In this paper, we extend the former model[31] to the eight-band case, taking into account the effects of electric and magnetic fields, to study the Rashba spin-orbit coupling in nanowires. The remainder of this paper is organized as follows: The calculation model is given in Sec. II. We calculate the electronic structure, Rashba coefficient, and effective g factors in Sec. III. Section IV is the conclusion.

II. THEORY MODEL AND CALCULATIONS

In the absence of electric and magnetic fields, the eight-band effective-mass Hamiltonian is represented in the Bloch function bases $|S\rangle\uparrow$, $|11\rangle\uparrow$, $|10\rangle\uparrow$, $|1-1\rangle\uparrow$, $|S\rangle\downarrow$, $|11\rangle\downarrow$, $|10\rangle\downarrow$, $|1-1\rangle\downarrow$ as

$$H_{eb} = H_{eb}^{01} + \begin{pmatrix} H_2 & 0 \\ 0 & H_2 \end{pmatrix}, \tag{1}$$

where H_{eb}^{01} contains k-independent terms and k-linear terms, and H_2 contains k-quadratic terms. H_{eb}^{01} is written as

$$H_{eb}^{01}=\begin{pmatrix} E_c & \frac{i}{\sqrt{2}}p_0k_+ & ip_0k_z & \frac{i}{\sqrt{2}}p_0k_- & 0 & 0 & 0 & 0 \\ -\frac{i}{\sqrt{2}}p_0k_- & E_v & 0 & 0 & 0 & 0 & 0 & 0 \\ -ip_0k_z & 0 & E_v-\lambda & 0 & 0 & -\sqrt{2}\lambda & 0 & 0 \\ -\frac{i}{\sqrt{2}}p_0k_+ & 0 & 0 & E_v-2\lambda & 0 & 0 & \sqrt{2}\lambda & 0 \\ 0 & 0 & 0 & 0 & E_c & \frac{i}{\sqrt{2}}p_0k_+ & ip_0k_z & \frac{i}{\sqrt{2}}p_0k_- \\ 0 & 0 & -\sqrt{2}\lambda & 0 & -\frac{i}{\sqrt{2}}p_0k_- & E_v-2\lambda & 0 & 0 \\ 0 & 0 & 0 & \sqrt{2}\lambda & -ip_0k_z & 0 & E_v-\lambda & 0 \\ 0 & 0 & 0 & 0 & -\frac{i}{\sqrt{2}}p_0k_+ & 0 & 0 & E_v \end{pmatrix}, \tag{2}$$

where λ is the k-independent spin-orbit coefficient, E_c and E_v are the band-edge energies, $E_c=E_g$, $E_v=0$, E_g is the band gap of bulk material, $p_0=\hbar\sqrt{E_P/2m_0}$, E_p is the matrix element of Kane's theory, and $k_\pm=k_x\pm ik_y$.

H_2 is written as

$$H_2=\frac{\hbar^2}{2m_0}\begin{pmatrix} P_e & 0 & 0 & 0 \\ 0 & -P_1 & -G & -F \\ 0 & -G^\star & -P_3 & -G \\ 0 & -F^\star & -G^\star & -P_1 \end{pmatrix}, \tag{3}$$

where

$$P_e=\gamma_c k_-k_+ +\gamma_c k_z^2, \tag{4a}$$

$$P_1=\frac{L'+M'}{2}k_-k_+ +M'k_z^2, \tag{4b}$$

$$P_3=M'k_-k_+ +L'k_z^2, \tag{4c}$$

$$F=\frac{L'-M'-N'}{4}k_+^2+\frac{L'-M'+N'}{4}k_-^2, \tag{4d}$$

$$F^*=\frac{L'-M'-N'}{4}k_-^2+\frac{L'-M'+N'}{4}k_+^2, \tag{4e}$$

$$G=\frac{1}{\sqrt{2}}N'k_-k_z, \tag{4f}$$

$$G^*=\frac{1}{\sqrt{2}}N'k_+k_z. \tag{4g}$$

γ_c, L', M', N' are given by

$$\gamma_c=\frac{m_0}{m_c}-\frac{E_p}{3}\left(\frac{2}{E_g}+\frac{1}{E_g+3\lambda}\right), \tag{5a}$$

$$L'=L-E_p/E_g, \tag{5b}$$

$$M'=M, \tag{5c}$$

$$N'=N-E_p/E_g, \tag{5d}$$

where m_c is the electron effective mass, and L, M, N are the Luttinger parameters.

In the spherical symmetry approximation, $L-M-N=0$, so that $L'-M'-N'=0$, and the first terms in Eqs. (4d) and (4e), respectively, are ignored.

We assume that the nanowires have cylindrical symmetry, the longitudinal axis is along the z direction, and the electrons and holes are confined laterally in an infinitely high potential barrier.

The longitudinal wave function is the plane wave, the lateral wave function is expanded in Bessel functions. The total envelope function including the electron and hole states is

$$\Psi_{J,k_z}=\sum_n \begin{pmatrix} e_{l,n,\uparrow}A_{l,n}J_l(k_n^l r)e^{il\theta} \\ b_{l-1,n,\uparrow}A_{l-1,n}J_{l-1}(k_n^{l-1}r)e^{i(l-1)\theta} \\ c_{l,n,\uparrow}A_{l,n}J_l(k_n^l r)e^{il\theta} \\ d_{l+1,n,\uparrow}A_{l+1,n}J_{l+1}(k_n^{l+1}r)e^{i(l+1)\theta} \\ e_{l+1,n,\downarrow}A_{l+1,n}J_{l+1}(k_n^{l+1}r)e^{i(l+1)\theta} \\ b_{l,n,\downarrow}A_{l,n}J_L(k_n^l r)e^{il\theta} \\ c_{l+1,n,\downarrow}A_{l+1,n}J_{l+1}(k_n^{l+1}r)e^{i(l+1)\theta} \\ d_{l+2,n,\downarrow}A_{l+2,n}J_{l+2}(k_n^{l+2}r)e^{i(l+2)\theta} \end{pmatrix} e^{ik_z z}, \tag{6}$$

where $J=l+1/2$ is the total angular momentum, and $A_{l,n}$ is the normalization constant,

$$A_{l,n} = \frac{1}{\sqrt{\pi} R J_{l+1}(\alpha_n^l)}. \tag{7}$$

In calculating the matrix elements of the Hamiltonian we can use the properties of the operators,

$$p_{\pm} J_l(kr) e^{il\theta} = \mp \frac{\hbar}{i} k J_{l\pm1}(kr) e^{i(l\pm1)\theta}. \tag{8}$$

Now we take into account the effects of electric and magnetic fields. For simplicity, we assume that the electric field is applied transversely, i.e., its direction is perpendicular to the z direction. As the nanowires have cylindrical symmetry, we assume that the transverse electric field is along the x direction (i.e., $\mathbf{E}_{ext} = \mathbf{E}_{ext}\hat{\mathbf{x}}$). Taking into account the dielectric effect, the electric field in the nanowires is

$$\mathbf{E} = \frac{2\epsilon_0}{\epsilon_r + \epsilon_0} \mathbf{E}_{ext} = \mathbf{E}_{nw}\hat{\mathbf{x}}, \tag{9}$$

where ϵ_r and ϵ_0 are the dielectric constants in and outside the nanowires, and $\hat{\mathbf{x}}$ is the unit vector along x direction. For air environment, $\epsilon_0 = 1$.

The electric field potential term is written as

$$V = e\mathbf{E} \cdot \mathbf{r} = eE_{nw}x = eE_{nw} r \cos\theta = \frac{1}{2} eE_{nw} r e^{i\theta} + \frac{1}{2} eE_{nw} r e^{-\theta}. \tag{10}$$

When the magnetic field is applied, the momentum operator changes into $\mathbf{p} \Rightarrow \mathbf{p} + e\mathbf{A}$, where $\mathbf{A}$ is the vector potential. For longitudinal magnetic field (B_z) we choose the symmetric gauge

$$\mathbf{A} = \left(-\frac{1}{2} B_z y, \frac{1}{2} B_z x, 0 \right). \tag{11}$$

For transverse magnetic field (B_x or B_y) we choose the Landau gauge

$$\mathbf{A} = (0,0,B_x y) \text{ or } (0,0,-B_y x). \tag{12}$$

The whole Hamiltonian in the presence of electric and magnetic fields is written as

$$H = H_{eb} + V + H_{asym} + H_{mm} + H_{Zeeman}, \tag{13}$$

where H_{asym}, H_{mm}, and H_{Zeeman} are the antisymmetric Hamiltonian,[52] magnetic-momentum Hamiltonian,[53] and spin-Zeeman-splitting Hamiltonian result, respectively.

With the method given above, we can do the numerical calculations on the Rashba spin-orbit effect. For comparison, we deduce the effective conduction band Hamiltonian term which includes the Rashba term.

First, we ignore the k-quadratic terms, and write the Schrödinger equation as

$$(H_{eb}^{01} + V) f = Ef, \tag{14}$$

$$f = (f_{e1}, f_{h1}, f_{h2}, f_{h3}, f_{e2}, f_{h4}, f_{h5}, f_{h6})^T, \tag{15}$$

where f_{ei} and f_{hj} are the electron and hole states. Eliminate f_{hj} in the above Schrödinger equation, we obtain

$$H_{temp} f_e = E f_e, \tag{16}$$

$$f_e = (f_{e1}, f_{e2})^T. \tag{17}$$

Adding the k-quadratic terms, averaging the transverse momentums, and ignoring the Stark shift, the effective conduction band Hamiltonian term is obtained as

$$H_{eff}(k_z) = E_g' + \frac{\hbar^2}{2m_0} \gamma_c' k_z^2 + \alpha(k_z) k_z \sigma_y, \tag{18}$$

$$\gamma_c' = \gamma_c + \frac{E_p}{3} \left(\frac{2}{E_g'} + \frac{1}{E_g' + 3\lambda} \right), \tag{19}$$

where $\alpha(k_z) k_z \sigma_y$ is the Rashba term and E_g' is the band gap of nanowires. We notice that $\gamma_c' < \frac{m_0}{m_c}$ because $E_g' > E_g$.

The Rashba spin-orbit splitting energy is

$$\begin{aligned} \Delta E &= 2\alpha(k_z) k_z \\ &= \frac{\hbar^2}{m_0} E_p \frac{\partial}{\partial x} \left(\frac{\lambda}{(E_g^* + \lambda - eE_{nw}x)(E_g^* + 2\lambda - eE_{nw}x) - 2\lambda^2} \right) k_z \\ &= \frac{\hbar^2}{m_0} E_p \frac{\lambda(2E_g^* + 3\lambda)}{E_g^{*2}(E_g^* + 3\lambda)^2} eE_{nw} k_z \\ &= \frac{\hbar^2}{m_0} E_p \frac{\lambda(2E_g^* + 3\lambda)}{E_g^{*2}(E_g^* + 3\lambda)^2} e \frac{2\epsilon_0}{\epsilon_r + \epsilon_0} E_{ext} k_z, \end{aligned} \tag{20}$$

and

$$\alpha(k_z) = \frac{\hbar^2}{2m_0} E_p \frac{\lambda(2E_g^* + 3\lambda)}{E_g^{*2}(E_g^* + 3\lambda)^2} e \frac{2\epsilon_0}{\epsilon_r + \epsilon_0} E_{ext}, \tag{21}$$

where

$$E_g^* = E_g' + \frac{\hbar^2}{2m_0} \gamma_c' k_z^2. \tag{22}$$

When we deduce Eq. (20), we take care of the sign. We see from Eq. (21) that $\alpha(k_z)$ is always positive. ΔE is not a linear function of k_z because E_g^* contains k_z-quadratic terms. When we deduce γ_c', we ignore the k_z-quadratic terms because γ_c' is defined in the small k_z range. In this range, $E_g^* \simeq E_g'$, ΔE has a linear relationship with k_z, and we can define a Rashba coefficient as

$$\alpha = \alpha(k_z = 0) = \frac{\hbar^2}{2m_0} E_p \frac{\lambda(2E_g' + 3\lambda)}{E_g'^2(E_g' + 3\lambda)^2} e \frac{2\epsilon_0}{\epsilon_r + \epsilon_0} E_{ext}. \tag{23}$$

III. RESULTS AND DISCUSSION

In this section, we calculate the electronic structure and Rashba coefficient of nanowires in the presence of electric and magnetic fields using the eight-band Kane model. We see from Eqs. (20) and (23) that the Rashba effect is larger when the band gap is smaller, so we choose the InSb material.

It is well known that Pfeffer and Zawadzki[10,11] have investigated the Rashba effect in quantum wells using the fourteen-band Kane model. The fourteen bands arise from $\Gamma_6^c(2)$, $\Gamma_8^v(4)$, $\Gamma_7^v(2)$, $\Gamma_8^c(4)$, and $\Gamma_7^c(2)$, which are double or

TABLE I. The parameters of InSb material.

m_c	L	M	N	E_P (eV)	E_g (eV)	Δ_{so} (eV)	ϵ_r
$0.0136m_0$	98.9	4.58	101.0	21.2	0.2352	0.81	16.8

fourfold degenerate in the absence of external fields. The eight-band Kane model whose eight bands arise from Γ_6^c, Γ_8^v, and Γ_7^v, is used when the higher order terms in k arising from the small coupling between Γ_6^c and Γ_8^c, Γ_7^c, and that between Γ_8^v, Γ_7^v and Γ_8^c, Γ_7^c can be ignored. In the eight-band Kane model, the large coupling between Γ_6^c and Γ_8^v, Γ_7^v is emphasized, and as this coupling actually dominate, so the Rashba coefficient calculated from this model is very close to the real value.

The parameters of InSb material used in this paper are listed in Table I. However, these parameters measured in the bulk material include some contributions, say, nonlocal character of the self-consistent potential, that are absent in narrow-gap nanostructures.[54,55] Therefore, using these parameters requires taking special precautions. The nonlocal contributions are

$$\Delta L = -21\delta_{nl}, \quad \Delta M = 3\delta_{nl}, \quad \Delta N = -24\delta_{nl}, \tag{24}$$

$$\Delta\alpha = -10\delta_{nl}, \quad \delta_{nl} = \frac{2}{15\pi\epsilon_r E_g}\sqrt{\frac{E_B E_p}{3}}, \tag{25}$$

where E_B=27.211 eV and ϵ_r is the dielectric constant.

We use the parameters K and b defined as follows to represent the electric field and magnetic field strengths,

$$K = \frac{eE_{ext}R}{\varepsilon_0}, \quad b = \frac{\hbar eB}{m_0\varepsilon_0}, \tag{26}$$

where

$$\varepsilon_0 = \frac{1}{2m_0}\left(\frac{\hbar}{R}\right)^2. \tag{27}$$

A. Effect of electric field

First of all, we show the electron states of InSb nanowires with radius of 8 nm in the presence of electric field along x direction with a strength of 7.44×10^7 V/m as functions of k_z in Fig. 1, especially the S states, detailed in Fig. 1(b). We see from Fig. 1(b) that at $k_z\neq0$ points, the doublets split. This is known as Rashba spin-orbit effect. Actually, all the doublets at $k_z\neq0$ points in Fig. 1(a) split, which cannot be seen clearly. From now on, we focus on the splitting of the lowest S states, which consist mainly of the n=1, l=0 state of the effective-mass envelope function multiplied with the Bloch state of the conduction-band bottom and the spin state. The symbols in Fig. 1(b) mainly indicate the spin state of the states. We see that when $k_z>0$, the state $\uparrow+i\downarrow$ is higher, and when $k_z<0$, it is lower. The result is just as expected, because the Rashba term is approximately written as $H_{Ra}=\alpha(k_z)k_z\sigma_y$ [see Eq. (18)], when $k_z>0$, $H_{Ra}\sim\sigma_y$, whose eigenvectors are $\uparrow+i\downarrow$ (eigenvalue 1) and $\uparrow-i\downarrow$ (eigenvalue −1), when $k_z<0$, $H_{Ra}\sim-\sigma_y$, whose eigenvectors are $\uparrow-i\downarrow$ (eigenvalue 1) and $\uparrow+i\downarrow$ (eigenvalue −1). The bands in Fig. 1(b) can be looked as a y directional spin-up ($\uparrow+i\downarrow$) band and a y directional spin-down ($\uparrow-i\downarrow$) band, which cross at k_z=0. If the nanowire is n-type doped and a current transports in it, the electrons will distribute nonequivalently, for example, more electrons distribute in the k_z-negative part than the k_z-positive part, then there will be more electrons distributes in the y directional spin-up band [see Fig. 1(b)], that to say, the electrons in the nanowire are spin polarized along the y direction, i.e., current brings spin polarization. It is already observed that current brings spin polarization in quantum wells.[16] We might suggest a similar experiments in nanowires.

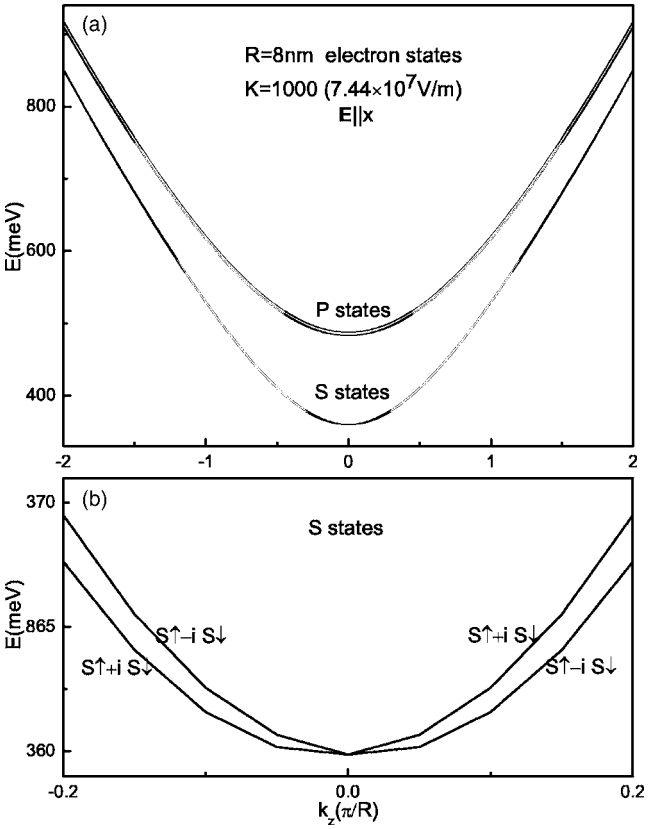

FIG. 1. Electron states of InSb nanowires with a radius of 8 nm in the presence of electric field along x direction with strength of 7.44×10^7 V/m as functions of k_z. (a) Electron states. (b) S states in details.

The spin-orbit splitting energy of InSb nanowires with a radius of 8 nm in the presence of electric field along x direction with strength of 7.44×10^7 V/m as a function of k_z is shown by the solid line in Fig. 2. We see that the splitting energy has the same sign with k_z, which is zero when k_z=0. The splitting energy is comparable to the quantum well case.[12] For positive k_z, the splitting energy increases as k_z increases at first, then interestingly decreases when k_z is large. The decreasing is caused by the k_z-quadratic term in the band energy [see Eqs. (22) and (20)], which is important in the large k_z range. We also show the empirical formula [Eq. (20)] result by the dotted line for comparison. We see that the empirical formula works very well in the small k_z

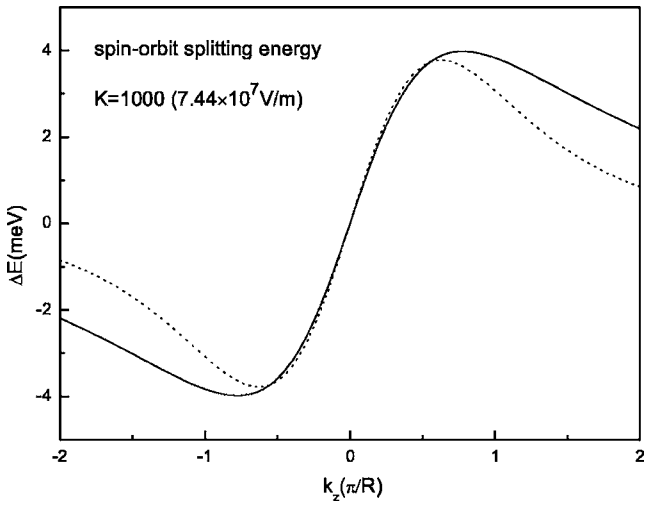

FIG. 2. Spin-orbit splitting energies of InSb nanowires with a radius of 8 nm in the presence of electric field along x direction with strength of 7.44×10^7 V/m as functions of k_z. The dotted lines are the results calculated from the empirical formula [Eq. (20)].

range, but not very good when k_z is large. This is because we ignore some higher order terms in k when we deduce the empirical formulas [see Eqs. (14)–(23)]. When k_z is small, the splitting energy is approximately a linear function of k_z, and it is convenient to use a Rashba coefficient to indicate this linear relationship [see Eq. (23)]. We show the Rashba coefficient of the $R=8$ nm case by the solid line in Fig. 3(a). We see that it is approximately a linear function of the external electric field. The empirical formula [Eq. (23)] result is shown by the dotted line. It is a strict linear function of electric field which can be seen from Eq. (23). The empirical result fits well. Figure 3(b) is the $R=24$ nm case. We see that the empirical result fits well in the small electric field range, but is defeated when E_{ext} is large. The Rashba coefficient

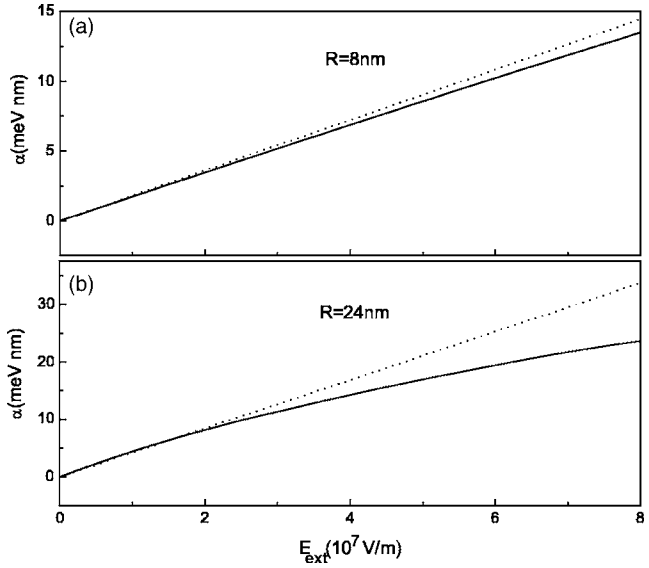

FIG. 3. Rashba coefficients of InSb nanowires as functions of E_{ext}. (a) $R=8$ nm. (b) $R=24$ nm. The dotted lines are the results calculated from the empirical formula [Eq. (23)].

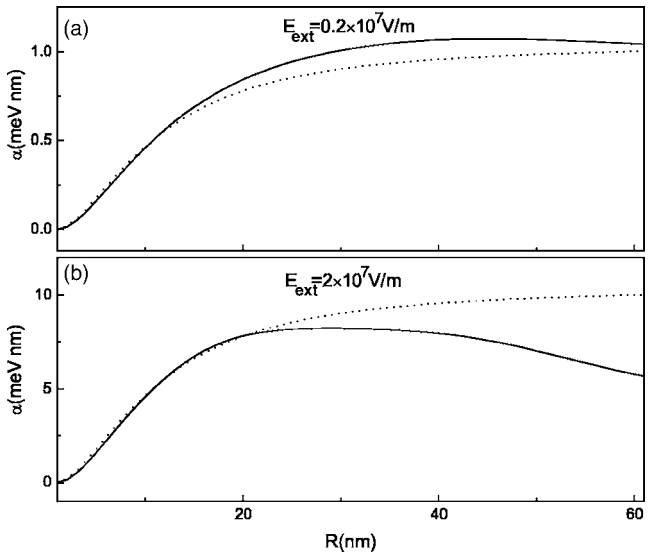

FIG. 4. Rashba coefficients of InSb nanowires as functions of R. (a) $E_{ext}=0.2\times10^7$ V/m. (b) $E_{ext}=2\times10^7$ V/m. The dotted lines are the results calculated from the empirical formula [Eq. (23)].

shows a saturating trend in the large E_{ext} range. This is due to the Stark effect which changes the state components, mixing the conduction-band states with the valence-band states. When we deduce the empirical formulas, we ignore the Stark effect. This can explain the deviation of the empirical results from the Kane model results. We also show the Rashba coefficients (solid lines) as well as the empirical results (dotted lines) in the presence of different electric field as functions of the radius in Fig. 4. We see that the Rashba coefficients increase at first, then decrease as the radius increases. In the larger electric field case [see Fig. 4(b)], the Rashba coefficient decreases beginning at a smaller radius. While the empirical results increase monotonously due to the decreasing of E_g' [see Eq. (23)] as the radius increases, they saturate when the radius is large and E_g' is very close to E_g [the band gap of bulk material]. The empirical formula works well only in the small R range, in which the increase of the Kane model results with increasing R can be explained similarly to the empirical results. The decrease of the Kane model results with increasing R in the large R range can also be explained by the Stark effect, as well as the deviation. As the band gap of InSb material is quite small, the mix of the conduction-band states and valence-band states due to the Stark effect is very large, so the deviations especially that in the larger electric field case are quite obvious. When the band gap of the material is large, the mix of the conduction-band states and valence-band states is small, and then the empirical formula [Eq. (23)] will work well in the whole R range. In the large R range, the Rashba coefficient saturates and does not change with R. This is similar to the case of experiment by Guzenko *et al.*[32]

B. Combined effect of electric and magnetic fields

The electron states and spin splitting energy of InSb nanowires with radius of 8 nm in the presence of electric field

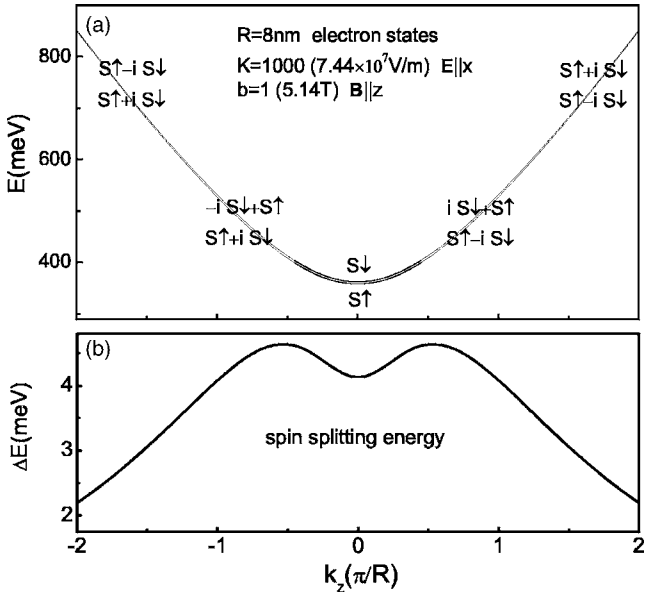

FIG. 5. Electron states and spin splitting energy of InSb nanowires with a radius of 8 nm in the presence of electric field along x direction with strength of 7.44×10^7 V/m and magnetic field along z direction with strength of 5.14 T as functions of k_z. (a) Electron states. (b) Spin splitting energy.

along x direction with strength of 7.44×10^7 V/m and magnetic field along z direction with strength of 5.14 T as functions of k_z are shown in Fig. 5. We see that the energy bands do not cross and the splitting energy is always positive, which is different from the case without magnetic field (see Figs. 1 and 2). In this case, the spin relative Hamiltonian term can be approximately written as $H_{spin}=\frac{1}{2}g_z\mu_B B\sigma_z+\alpha(k_z)k_z\sigma_y$. When $k_z=0$, $H_{spin}=\frac{1}{2}g\mu_B B\sigma_z$, the spins parallel or antiparallel to the z direction split, and when $|k_z|$ is quite large, $H_{spin}\sim\alpha(k_z)k_z\sigma_y$, the spins parallel or antiparallel to the y direction split. The detailed state components are shown in Fig. 5(a). We see that, when $k_z=0$, the two states are mainly the two eigenstates of σ_z; when $|k_z|$ is quite large, the two states are mainly the two eigenstates of σ_y. When $|k_z|$ changes from zero to a quite large value, the state components changes smoothly, i.e., the spin directions of the bands, respectively, changes from parallel or antiparallel to the z direction to parallel or antiparallel to the y direction smoothly. The case in which the magnetic field is along the x direction (i.e., parallel to the electric field) is quite similar to Fig. 5 and not shown here. In this case, $H_{spin}=\frac{1}{2}g_x\mu_B B\sigma_x+\alpha(k_z)k_z\sigma_y$, and when $k_z=0$, the spins parallel or antiparallel to the x direction split. The common point of these two cases is that the spin splitting due to the electric field (Rashba spin-orbit splitting) and that due to the magnetic field (spin Zeeman splitting) are in different directions. The Rashba spin-orbit splitting is approximately a linear function of k_z, while the spin Zeeman splitting is approximately independent of k_z. So as k_z increases from 0 to a large value, the spin splitting direction changes.

The electron states and spin splitting energy of InSb nanowires with radius of 8 nm in the presence of electric field along x direction with strength of 7.44×10^7 V/m and magnetic field along y direction with strength of 5.14 T as functions of k_z are shown in Fig. 6. It is interesting to notice that this case is quite different from the above two cases, the k_z-positive and negative parts of the energy bands are not symmetrical, and the energy bands cross at a k_z-positive point. We can see from the detailed state components in Fig. 6(a) that the spins always split along the y direction. The spin splitting energy changes from negative to positive value with increasing k_z, as shown in Fig. 6(b). The most important different point of this case from the above two cases is that the spin splitting due to the electric field and that due to the magnetic field are in the same direction. In this case, the spin relative Hamiltonian is approximately written as $H_{spin}=\left[\frac{1}{2}g_y\mu_B B+\alpha(k_z)k_z\right]\sigma_y$. In InSb nanowires with $R=8$ nm, $g_y<0$, which can also be seen from the state symbols at $k_z=0$ point in Fig. 6(a) where $H_{spin}=\frac{1}{2}g_y\mu_B B\sigma_y$ and y directional spin-up state is lower. If we assume that $\frac{1}{2}g_y\mu_B B+\alpha(k_{z0})k_{z0}=0$, then at the critical $k_z=k_{z0}$ point, $H_{spin}=0$ and the spin splitting energy is zero, as shown in Fig. 6(b). We can define an effective g factor as $g^*=\Delta E/\mu_B B$. At the critical k_z point, $g^*=0$. The effective g factor of InSb nanowires with radius of 8 nm in the presence of electric field along x direction and magnetic field ($b=1$) along y direction as a function of k_z and K is shown in Fig. 7. We see that when $K=0$ the k_z-positive and negative parts are symmetrical, the smallest g^* point is at $k_z=0$. As K increases, the asymmetry happens, the smallest g^* point moves to negative k_z direction. The reason is similar to that of the asymmetry of spin splitting energy, and the smallest point is similar to that in Fig. 6(b). There are negative and positive g^* values in Fig. 7, and also many zero values, with which we can obtain the critical

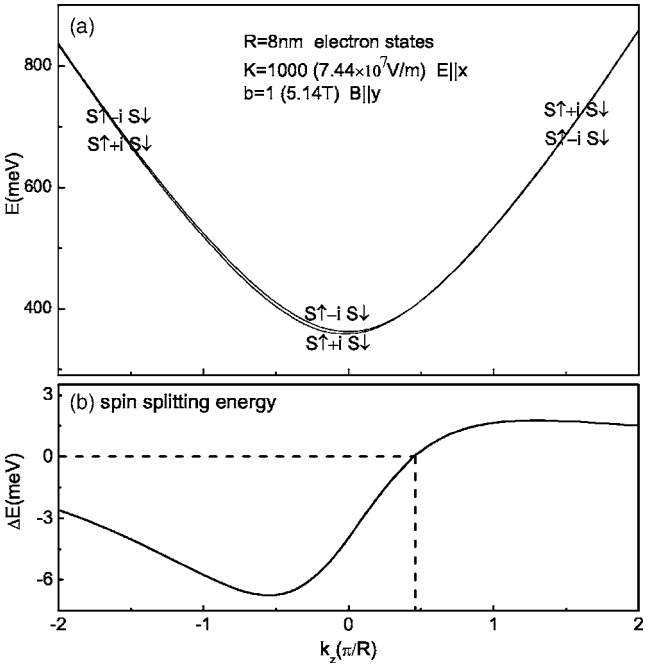

FIG. 6. Electron states and spin splitting energy of InSb nanowires with a radius of 8 nm in the presence of electric field along x direction with strength of 7.44×10^7 V/m and magnetic field along y direction with strength of 5.14 T as functions of k_z. (a) Electron states. (b) Spin splitting energy.

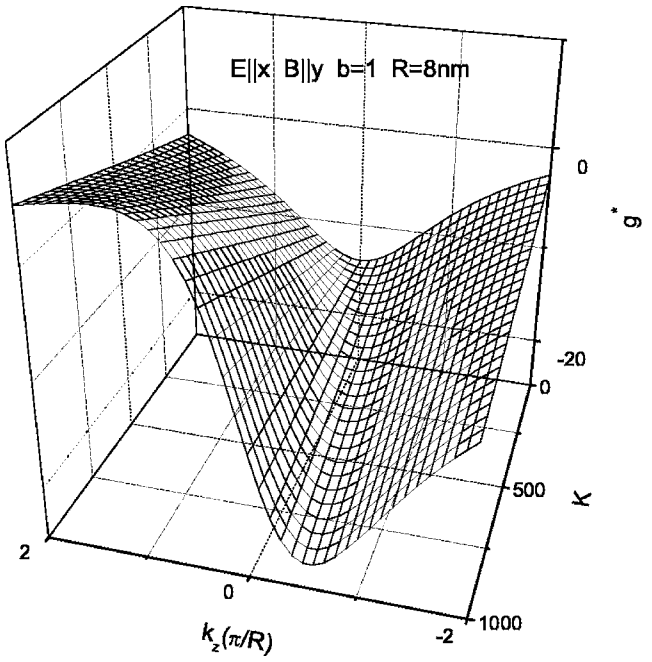

FIG. 7. Effective g factor of InSb nanowires with a radius of 8 nm in the presence of electric field along x direction and magnetic field ($b=1$) along y direction as a function of k_z and K.

k_z points at different electric field. We see that the critical k_z points decrease with increasing K because the Rashba spin-orbit splitting dominates at a smaller k_z when K is larger. The effective g factor at $k_z=0$ point does not change with the electric field because H_{spin} $\left(=\frac{1}{2}g_y\mu_B B\sigma_y\right)$ is independent of the electric field.

IV. CONCLUSIONS

The Rashba spin-orbit coupling in InSb nanowires caused by the structure inversion asymmetry (SIA) which is brought by the external transverse electric field in the case of this paper is investigated. Similar to the quantum well case, in small k_z range, the Rashba spin-orbit splitting energy is a linear function of k_z, so we define a Rashba coefficient. We deduce some empirical formulas of the Rashba coefficient and spin-orbit splitting energy and compare the results with the effective-mass calculations. The empirical formulas fit well when R, k_z, and K are all not very large. It is interesting to find that the Rashba spin-orbit splitting energy decreases as k_z increases when k_z is large due to the k_z-quadratic term in the band energy [see Eq. (22) and (20)]. The Rashba coefficient increases with increasing electric field, and shows a saturating trend when the electric field is large. As the radius increases, the Rashba coefficient increases at first, and then decreases. The effects of magnetic fields along different directions are discussed. The cases that the magnetic field is along the wire direction or the electric field direction are similar. The spin state in an energy band changes smoothly as k_z changes. The case that the magnetic field is perpendicular to the wire direction and the electric field direction are quite different from the above two, the k_z-positive and negative parts of the energy bands are not symmetrical, and the energy bands with different spins cross at a k_z-nonzero point, where the effective g factor is zero. The tunable (by electric field or magnetic field) zero g factor is useful in spintronics.[56] The most important different point of the last case from the above two cases is that the spin splittings due to the electric field and magnetic field, respectively, are in same direction or not. The tunable Rashba spin-orbit coupling brought by transverse electric field will strongly influences the longitudinal spin-dependent transport properties. One-dimensional Datta-Das spin-FET and spin filter[51] can be designed. Spin polarization brought by current which is similar to the quantum well case[16] can be observed.

ACKNOWLEDGMENTS

This work was supported by the National Natural Science Foundation Grants No. 90301007 and No. 60521001, and the special funds for Major State Basic Research Project No. G001CB3095 of China.

[1] G. A. Prinz, Science **282**, 1660 (1998).
[2] S. A. Wolf *et al.*, Science **294**, 1488 (2001); *Semiconductor Spintronics and Quantum Computation*, edited by D. D. Awschalom, D. Loss, and N. Samarth (Springer, Berlin, 2002).
[3] S. Datta and M. Das, Appl. Phys. Lett. **56**, 665 (1990).
[4] J. C. Egues, G. Burkard, and D. Loss, Appl. Phys. Lett. **82**, 2658 (2003).
[5] J. Schliemann, J. C. Egues, and D. Loss, Phys. Rev. Lett. **90**, 146801 (2003).
[6] E. I. Rashba, Sov. Phys. Solid State **2**, 1109 (1960).
[7] Y. A. Bychkov and E. I. Rashba, JETP Lett. **39**, 78 (1984).
[8] Y. A. Bychkov and E. I. Rashba, J. Phys. C **17**, 6039 (1984).
[9] S. D. Ganichev, V. V. Bel'kov, L. E. Golub, E. L. Ivchenko, Petra Schneider, S. Giglberger, J. Eroms, J. De Boeck, G. Borghs, W. Wegscheider, D. Weiss, and W. Prettl, Phys. Rev. Lett. **92**, 256601 (2004).
[10] P. Pfeffer and W. Zawadzki, Phys. Rev. B **52**, R14332 (1995).
[11] W. Zawadzki and P. Pfeffer, Semicond. Sci. Technol. **19**, R1 (2004).
[12] W. Yang and K. Chang, Phys. Rev. B **73**, 113303 (2006).
[13] Th. Schäpers, G. Engels, J. Lange, Th. Klocke, M. Hollfelder, and H. Lüth, J. Appl. Phys. **83**, 4324 (1998).
[14] B. Jusserand, D. Richards, G. Allan, C. Priester, and B. Etienne, Phys. Rev. B **51**, 4707 (1995).
[15] X. C. Zhang, A. Pfeuffer-Jeschke, K. Ortner, V. Hock, H. Buhmann, C. R. Becker, and G. Landwehr, Phys. Rev. B **63**, 245305 (2001).
[16] C. L. Yang, H. T. He, Lu Ding, L. J. Cui, Y. P. Zeng, J. N. Wang, and W. K. Ge, Phys. Rev. Lett. **96**, 186605 (2006).
[17] F. E. Meijer, A. F. Morpurgo, T. M. Klapwijk, T. Koga, and J.

Nitta, Phys. Rev. B **70**, 201307(R) (2004).
[18] M. Governale, Phys. Rev. Lett. **89**, 206802 (2002).
[19] E. Tsitsishvili, G. S. Lozano, and A. O. Gogolin, Phys. Rev. B **70**, 115316 (2004).
[20] C. F. Destefani, S. E. Ulloa, and G. E. Marques, Phys. Rev. B **69**, 125302 (2004).
[21] C. L. Romano, S. E. Ulloa, and P. I. Tamborenea, Phys. Rev. B **71**, 035336 (2005).
[22] I. L. Aleiner and Vladimir I. Fal'ko1, Phys. Rev. Lett. **87**, 256801 (2001).
[23] J. Könemann, R. J. Haug, D. K. Maude, V. I. Fal'ko, and B. L. Altshuler, Phys. Rev. Lett. **94**, 226404 (2005).
[24] Matt Law, Joshua Goldberger, and Peidong Yang, Annu. Rev. Mater. Res. **34**, 83 (2004).
[25] J. A. Ascencio, P. Santiago, L. Rendon, and U. Pal, Appl. Phys. A: Mater. Sci. Process. **A78**, 5 (2004).
[26] Hae Gwon Lee, Hee Chang Jeon, Tae Won Kang, and Tae Whan Kim, Appl. Phys. Lett. **78**, 3319 (2001).
[27] S. V. Zaitsev-Zotov, Yu A. Kumzerov, Yu A. Firsov, and P. Monceau, J. Phys.: Condens. Matter **12**, L303 (2000).
[28] S. Banerjee, A. Dan, and D. Chakravorty, J. Mater. Sci. **37**, 4261 (2002).
[29] N. Mingo, Appl. Phys. Lett. **84**, 2652 (2004).
[30] S. V. Zaitsev-Zotov, Yu A. Kumzerov, Yu A. Firsov, and P. Monceau, JETP Lett. **77**, 135 (2003).
[31] X. W. Zhang and J. B. Xia, J. Phys.: Condens. Matter **18**, 3107 (2006).
[32] V. A. Guzenko, J. Knobbe, H. Hardtdegen, Th. Schäpers, and A. Bringer, Appl. Phys. Lett. **88**, 032102 (2006).
[33] S. Ihnatsenka and I. V. Zozoulenko, Phys. Rev. B **73**, 075331 (2006).
[34] M. Governale and U. Zülicke, cond-mat/0407036, Solid State Commun. (to be published).
[35] E. A. de Andrada e Silva and G. C. La Rocca, Phys. Rev. B **67**, 165318 (2003).
[36] Wolfgang Häusler, Phys. Rev. B **63**, 121310(R) (2001).
[37] Wolfgang Häusler, Phys. Rev. B **70**, 115313 (2004).
[38] Th. Schäpers, J. Knobbe, and V. A. Guzenko, Phys. Rev. B **69**, 235323 (2004).
[39] V. Gritsev, G. I. Japaridze, M. Pletyukhov, and D. Baeriswyl, Phys. Rev. Lett. **94**, 137207 (2005).
[40] Marco G. Pala, Michele Governale, Ulrich Zülicke, and Giuseppe Iannaccone, Phys. Rev. B **71**, 115306 (2005).
[41] Francisco Mireles and George Kirczenow, Phys. Rev. B **64**, 024426 (2001).
[42] L. G. Wang, Kai Chang, and K. S. Chan, J. Appl. Phys. **99**, 043701 (2006).
[43] X. F. Wang, Phys. Rev. B **69**, 035302 (2004).
[44] Dario Bercioux, Michele Governale, Vittorio Cataudella, and Vincenzo Marigliano Ramaglia, Phys. Rev. B **72**, 075305 (2005).
[45] S. Debald and B. Kramer, Phys. Rev. B **71**, 115322 (2005).
[46] J. Knobbe and Th. Schäpers, Phys. Rev. B **71**, 035311 (2005).
[47] Yue Yu, Yuchuan Wen, Jinbin Li, Zhaobin Su, and S. T. Chui, Phys. Rev. B **69**, 153307 (2004).
[48] Llorenç Serra, David Sánchez, and Rosa López, Phys. Rev. B **72**, 235309 (2005).
[49] Yuriy V. Pershin, James A. Nesteroff, and Vladimir Privman, Phys. Rev. B **69**, 121306(R) (2004).
[50] Yuriy V. Pershin and Carlo Piermarocchi, Appl. Phys. Lett. **86**, 212107 (2005).
[51] P. Štreda and P. Šeba, Phys. Rev. Lett. **90**, 256601 (2003).
[52] J. M. Luttinger, Phys. Rev. **102**, 1030 (1956).
[53] X. W. Zhang and J. B. Xia, Phys. Rev. B **72**, 075363 (2005).
[54] Y. H. Zhu, X. W. Zhang, and J. B. Xia, Phys. Rev. B **73**, 165326 (2006).
[55] Al. L. Efros and M. Rosen, Phys. Rev. B **58**, 7120 (1998).
[56] Kai Chang, J. B. Xia, and F. M. Peeters, Appl. Phys. Lett. **82**, 2661 (2003).